minerals

MDPI

Article

Modified Alkali Activated Zeolite Foams with Improved Textural and Mechanical Properties

Kateřina Hrachovcová *, Zdeněk Tišler, Eliška Svobodová and Jan Šafář

Unipetrol Centre for Research and Education, a.s., Areál Chempark 2838, Záluží 1, 436 70 Litvínov, Czech Republic; zdenek.tisler@unicre.cz (Z.T.); Eliska.Svobodova@unicre.cz (E.S.); Jan.Safar@unicre.cz (J.Š.)

* Correspondence: katerina.hrachovcova@unicre.cz

Received: 27 April 2020; Accepted: 23 May 2020; Published: 25 May 2020

Abstract: Natural zeolites are crystalline hydrated alkali metal and alkaline earth metal aluminosilicates with unique ion-exchange and sorption properties. The exceptional structure of pores gives natural zeolites several application possibilities, especially for water treatment and construction. For a wider use of natural zeolites, such as catalysis, properties—especially chemical, textural, and mechanical—need to be modified. In this study, the basic natural zeolite foam was synthesized by alkali activation of natural zeolite with an activator (KOH + Na_2SiO_3) and foamed by hydrogen peroxide solution. Other foams were prepared by a partial replacement of the natural zeolite with CaO, MgO, and metakaolin (MK) and alkali activated and foamed in the same manner as the basic natural zeolite foam. Other properties of the foams were modified by acid leaching. The aim of the study was to compare the basic alkali activated zeolite foam with the CaO, MgO, and MK modified zeolite foams and determine the effect of the CaO, MgO, and MK modification and the subsequent leaching of the alkali activated zeolite foams on the textural, mechanical, and chemical properties. Properties of alkali activated zeolite foams were determined by Hg porosimetry, N_2 physisorption, NH_3-TPD, XRF, XRD, and strength analyses. From the data, it is apparent that all modified samples have an increase of pore volume in the mesoporous region and the partial replacement by MgO or CaO significantly increased surface area up to 288.2 m^2/g while increasing the strength several times. The obtained data showed an improvement in properties and extension of the potential applicability of modified zeolite foams in the chemical industry, especially for catalytic and sorption applications.

Keywords: natural zeolite; clinoptilolite; alkali activation; acid leaching; inorganic foam

1. Introduction

Natural zeolites are an essential component of volcanogenic sedimentary rock and volcanic tuffs. Natural zeolites have been used for many years and have found a lot of applications in construction industry, soil remediation, agriculture, wastewater treatment, and energy [1]. Zeolites are naturally occurring aluminosilicates containing pores with adsorption and ion-exchange capabilities [2]. These aluminosilicates have a three-dimensional structure of SiO_4 and AlO_4 tetrahedra. These are interconnected by sharing all of the peak oxygen to form channels and cages connected to each other [3]. Channels contain alkali (Na, K) and/or alkaline earth (Ca, Mg) cations and mobile water molecules. There are only a few natural zeolites that are found in quantity and purity to be used in the industry. The most common zeolites are heulandite (clinoptilolite) and mordenite, which are rich in silica [4].

Natural zeolite containing clinoptilolite is an outstanding material that is added as an additive to cement [5]. The usage of natural zeolite enhances the strength of concrete and is more efficient than fly ash and less efficient than silica fume on concrete strength [6]. Studies show that the replacement of cement by natural zeolite can improve the mechanical properties of cement and concrete composite [5].

The microporous structure of natural zeolite is blocked by the cations present. Furthermore, the pores can be blocked by amorphous SiO_2 structures formed by the crystallization of zeolite rocks, and accompanying minerals, such as spar, mica, and clays [7]. It is clear that for more efficient use of natural zeolites as catalysts, it is necessary to improve the textural properties—e.g., access to the primary structure of clinoptilolite (access to micropores). Therefore, a porosity modification is often used to improve zeolite properties. An increase of zeolite mesoporosity can be achieved, for example, by post-treatment (acid leaching) modification of the calcined zeolite to support dealumination [8]. This procedure generates rare properties, such as relatively high thermal stability and high specific surface area. Thanks to these improved properties, zeolites can be used in heterogeneous catalysis or sorption applications [9].

Post-synthesis modifications, such as acid leaching, lead to the removal of framework aluminum (FAl) and improve the properties of natural zeolite, especially Si/Al [10]. Dealumination leads to the removal of accompanying minerals and cations from the micropores and thereby purify them.

Geopolymerization is a chemical reaction where minerals, that contain aluminosilicates, are integrated [11]. The source of silica and alumina, which is easily soluble in the alkaline medium, work as a source of geopolymer precursors and thus suitable for geopolymerization [12]. Alkali activated materials form only amorphous structure and do not form crystalline structure, as zeolites do [13]. Alkali activation is a polycondensation reaction and leads to the formation of new structures in which the resulting negative charge is compensated by cations (Na^+ or K^+) from the alkaline activator (KOH and Na_2SiO_3). The alkaline activation of the zeolite may consist of steps such as raw material dissolution, nucleation and amorphous gel formation, and solidification and hardening [9].

Alkaline activation results in an amorphous N(K)–A–S–H gel (N = Na_2O, K = K_2O, A = Al_2O_3, S = SiO_2, H = H_2O) [14]. In the case of adding CaO or MgO to the natural zeolite and subsequent alkaline activation, CaO and MgO reacts with Na_2SiO_3 and forms CSH and MSH phase, respectively. Alkali activated materials have several known advantages, such as exceptional mechanical strength, acid and fire resistance, long term durability, fast setting, and low thermal conductivity. Therefore, these materials are mainly used in the construction, and thermal and heat insulation industries, but they are also used for several applications, such as catalysts and membranes [15].

In the present work, we report the difference between basic alkali activated zeolite foam and CaO, MgO, and MK modified alkali activated zeolite foams. We observed the effect of CaO MgO and MK modification and subsequent leaching on the strength and texture characteristics of materials. The characterization of the materials using a series of techniques (such as N_2 physisorption, Hg porosimetry, temperature programmed desorption of ammonia (NH_3-TPD), X-ray fluorescence (XRF), and X-ray powder diffraction (XRD) methods) were undertaken in order to provide important information about their behavior, composition, structure, mechanical, and chemical properties. Such information is going to be very useful for further development of catalysts and for use in sorption applications.

2. Materials and Method

2.1. Materials

In this study, we used analytical grade potassium hydroxide, calcium oxide, magnesium oxide, H_2O_2 (30 wt %), HCl (35 wt %). These chemicals were provided by Lach-Ner s.r.o. (Neratovice, Czech Republic) in a pro analysis (p.a.) purity. Water glass (Na_2SiO_3) with silicate modulus 3.22 was obtained from Labar s.r.o. (Ústí nad Labem, Czech Republic) in a technical grade purity. The natural zeolite ECO 50 (Zeocem a.s., Bystré, Slovakia) and the Metakaoline MK05 (České lupkové závody a.s., Nové Strašecí, Czech Republic) were used for the preparation of the samples.

Powdered natural zeolite (NZ) contains at least 85 wt % of clinoptilolite, 9 wt % of clays, 4 wt % of feldspar, and 2 wt % of mica. Using the BET method, a specific surface area of 24 m^2/g was measured for this powdered natural zeolite. The chemical compositions of natural zeolite and metakaolin obtained by the XRF method are shown in Table 1.

Table 1. Chemical composition of natural zeolite and metakaolin

Sample	Chemical Composition (wt %)										Si/Al Ratio **
	SiO_2	Al_2O_3	K_2O	Fe_2O_3	CaO	Na_2O	MgO	TiO_2	LOI *	SUM	
NZ	66.80	10.98	4.23	1.97	4.23	0.22	0.65	0.24	9.97	99.29	5.16
MK05	56.71	37.57	0.89	0.79	0.20	0.00	0.39	0.59	1.38	98.52	1.26

* LOI is the loss on ignition at 900 °C; ** Si/Al ratio is the molar ratio of Si to Al.

2.2. Synthesis and Post-Synthesis Modifications of Zeolite Foams

Zeolite foams were prepared by mixing the powdered natural zeolite (NZ) with KOH solution representing an alkaline activator, and with H_2O_2 representing a foaming agent ingredient. Demineralized water, Na_2SiO_3, and 40% KOH solution were used to prepare the alkaline activator. The resulting silicate modulus $M_s = (SiO_2)/(Me_2O)$ of the alkaline activator was 1.51. The value of the water coefficient (w), which is the weight of water in the mixture to the weight of natural zeolite, was 0.7. Other parameters of alkali activated mixture were the content of Me_2O alkali (Me_2O = 8.2 wt %, Me = K + Na) and the molar ratio (Na_2O:K_2O = 0.56). Into the homogenized mixture the foaming agent (30 wt % H_2O_2) was added, so in the final mixture H_2O_2 was 0.125 wt %.

The alkali activated mixture with the added foaming agent was poured into forms with a diameter of 5 mm. The resulting pellets were activated for 48 h at 50 °C. Then, the pellets were placed in a plastic bag and allowed to age for a month at ambient conditions. The prepared sample was denoted AA-S. Another foams were prepared by partial replacement of natural zeolite by CaO, MgO, and metakaolin (MK) and then alkali activated, foamed, and shaped in the same manner as natural zeolite without additives described above. The prepared samples were denoted as additional compound (weight %) as follows CaO(2.5), CaO(6.25), CaO(12.5), MgO(2.5), MgO(6.25), MgO(12.5), MK(2.5), MK(6.25), and MK(12.5).

The prepared foam pellets (samples S) were first dried overnight at 120 °C, and then, part of them was leached at 80 °C using 0.1 M (samples denoted D1) or 3 M HCl (samples denoted D2) for 6 h. The foam/solution ratio (g/mL) was 1:20 for all samples. Finally, the samples were washed with demineralized water until a neutral pH was reached and then dried at 120 °C overnight.

2.3. Characterisation

The chemical composition of the natural zeolite and the prepared samples was determined by X-ray fluorescence analysis (XRF) using the S8 Tiger (Bruker AXS GmbH, Karlsruhe, Germany) with Rh cathode and Spectra plus software (Version 3).

The crystal phase identification was determined by X-ray diffraction (XRD) analysis using D8 Advance ECO powder diffractometer (Bruker AXS GmbH, Karlsruhe, Germany) with CuKα radiation (λ = 1.5406 Å). The resolution of 0.02° and the period of 0.5 were used. The crystallinity was determined at 2θ 9.9° [020]. The measurements were performed over a 2θ range of 5° to 70° and evaluated by the Diffrac.Eva software (Bruker AXS GmbH, Karlsruhe, Germany) using the Powder Diffraction File Database (PDF 4+ 2018, International Centre for Diffraction Data, Newtown Square, PA, USA).

The textural properties were defined by N_2 physisorption and mercury porosimetry measurement. Samples for N_2 physisorption measurement were first degassed under vacuum at 110 °C for 16 h, and then the adsorption and desorption isotherms were measured at −196 °C. Degassing and the measurement were performed using Autosorb iQ (Quantachrome Instruments, Boynton Beach, FL, USA). The specific surface area was calculated by the Brunauer–Emmett–Teller (BET) method in the pressure range of 0.05–0.30 p/p_0. In the case of samples where micropores were present, a linear range for the S_{BET} was in the range of 0.005 to 0.01 p/p_0. The total pore area, pore-size distribution, and microporous and mesoporous volumes were determined by the non-local density functional theory (NLDFT).

Macroporous properties were determined using mercury (Hg) porosimetry (AutoPore IV 9510, Micromeritics Instrument Corporation, Norcross, GA, USA). Samples for mercury porosimetry were

dried under vacuum at 110 °C for 16 h. The measurement was performed in two steps. The first step was the low-pressure analysis (0 to 345 kPa) and the second step was the high-pressure analysis (from atmospheric pressure to 414 MPa).

The strength in the cutting edge was defined using UMZ-3k (Micro-Epsilon, Bechyně, Czech Republic) with a corresponding trapezoidal flat blade attachment (area size 1 mm). Maximum strength parameter 375 N, load speed 10 mm/min. Statistical data processing was used to obtain the final results.

The number type and strength of the acid sites on the surface of the samples were determined by ammonia temperature programmed desorption (NH_3-TPD) using Autochem 2950 HP device (Micromeritics Instrument Corporation, Norcross, GA, USA). A pellet (100 mg) was weighed into a quartz tubular reactor. The inside of the reactor was a quartz wool plug. The first step was the pre-treatment of the sample. Then, the sample was saturated with ammonia. NH_3 molecules physically adsorbed on the surface were removed by flushing the sample out in the flow of helium. The NH_3 desorption was performed by passing He through the reactor and by the increasing temperature. The desorbed NH_3 in the outlet gas was detected using a thermal conductivity detector (TCD). The amount of weak and strong acid sites was estimated by integrating the low- and high-temperature desorption peak areas, respectively.

Steps of NH_3-TPD analysis:

1. Pre-treatment:
    a. The flow of pure He (flow rate 25 mL/min)
    b. Heating to 450 °C (heating rate 10 °C/min, isotherm 30 min)
    c. Cooling to 100 °C
2. Sorption:
    a. Flowing gas mixture (90 vol. % of He and 10 vol. % of ammonia, flow rate 25 mL/min, for 30 min)
3. Removing of physically adsorbed molecules:
    a. The flow of pure He (flow rate 25 mL/min, for 30 min)
4. Desorption:
    a. He through the reactor (25 mL/min)
    b. Increasing temperature from 100 °C to 450 °C (heating rate 10 °C/min)

3. Results and Discussion

The chemical composition of the samples was determined by the X-ray fluorescence (XRF) analysis (Figure 1). The results showed that leaching with different strength of HCl significantly affected the resulting chemical properties of all samples. The higher concentration of HCl used caused an increase in the proportion of leached components from the zeolite foam indicated by the M_{Si} parameter (characterized by the removal degree of elements from the material) and the Si/Al ratio. Leaching using 0.1 M acid led to the removing of Na and a slight loss of K and Ca. When using 3M HCl, a more pronounced loss of K, Na, and Ca was observed and also the elements—such as Al, Mg, and Fe—were removed.

When the natural zeolite was partially replaced by MgO and CaO, followed by leaching by 0.1M acid, only a slight decrease of the Mg and the Ca was observed (Table A1 (Appendix A)). By leaching using 3M acid, all Mg and Ca were removed from the material. Samples with partial replacement of natural zeolite (MgO, CaO, and MK) showed, after the subsequent leaching, almost identical elemental composition results.

For the D1 samples, there was only a small increase in the M_{Si} parameter and the Si/Al ratio remained almost unchanged. The M_{Si} decrease for the MgO and CaO samples was due to the external addition of

MgO and CaO to mixtures that D1 leaching did not remove. In D2 samples, the Si/Al ratio increased two times and the M_{Si} parameter increased up to ten times due to the primary removal of a large amount of sodium and potassium (Figure 2). MgO(12.5)-modified zeolites had the largest increase in Si/Al ratio using 3M HCl. After Mg removal, there was probably more Al available for the acid and therefore easier to remove. A significant increase in Si/Al ratio was also evident in the CaO (6.25)-D2 modified zeolite. There CaO (and also MgO) reacts with the water glass to silicate or to CSH (or MSH in the case of MgO) phase containing wollastonite ($CaSiO_3$ detected in the XRD). The lowest Si/Al ratio had the alkali activated sample (AA) without additionally added compounds. When leaching with 3 M HCl, the M_{Si} parameter increased up to eight times in most modified samples (Figure 2).

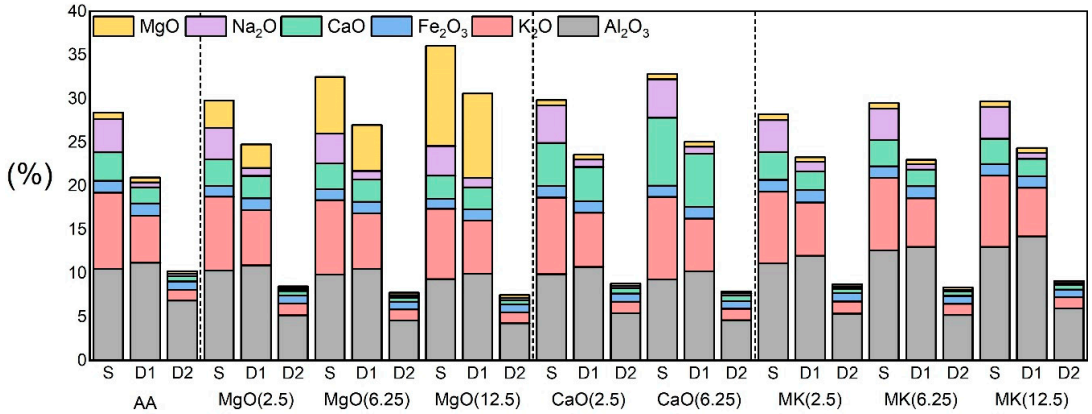

Figure 1. Chemical composition of samples (silicon is up to 100%).

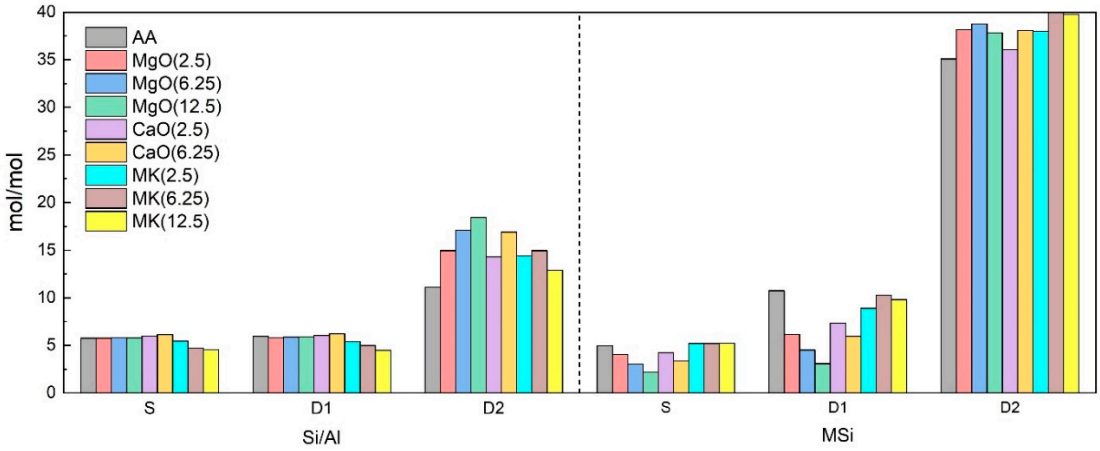

Figure 2. Si/Al ratio and M_{Si} parameter of samples.

The X-ray powder diffraction (XRD) method was used to determine the crystalline structure that showed the crystalline phase of clinoptilolite with classic reflections at 2θ 9.9°, 11.2°, 17.5°, 22.4° and other minor minerals, such as feldspars, clays, and mica (Figure 3a,b).

Alkaline activation of natural zeolite (AA) slightly increased the intensity (7%) of the reflection of 11.2° 2θ, [200] due to the higher electron density in a given crystal plane caused by the presence of Na and K cations [13]. On the other hand, AA activation also resulted in an approximately 60% decrease in the intensity of reflection of 9.9° 2θ, [020] (Table 2). In the MgO(2.5)–MgO(6.25) samples, only the low MgO (PDF 65-0476) intensities of the samples at 42.9° 2θ were evident. Diffractograms also showed insignificant intensities associated with the CSH phase ($CaO–SiO_2–H_2O$), consisting of wollastonite (PDF 72-2297), resulting from the reaction of CaO with the alkaline activator (sodium silicate). In the MK samples were visible low intensities of mullite (PDF 79-1458) coming from the raw material—metakaolin.

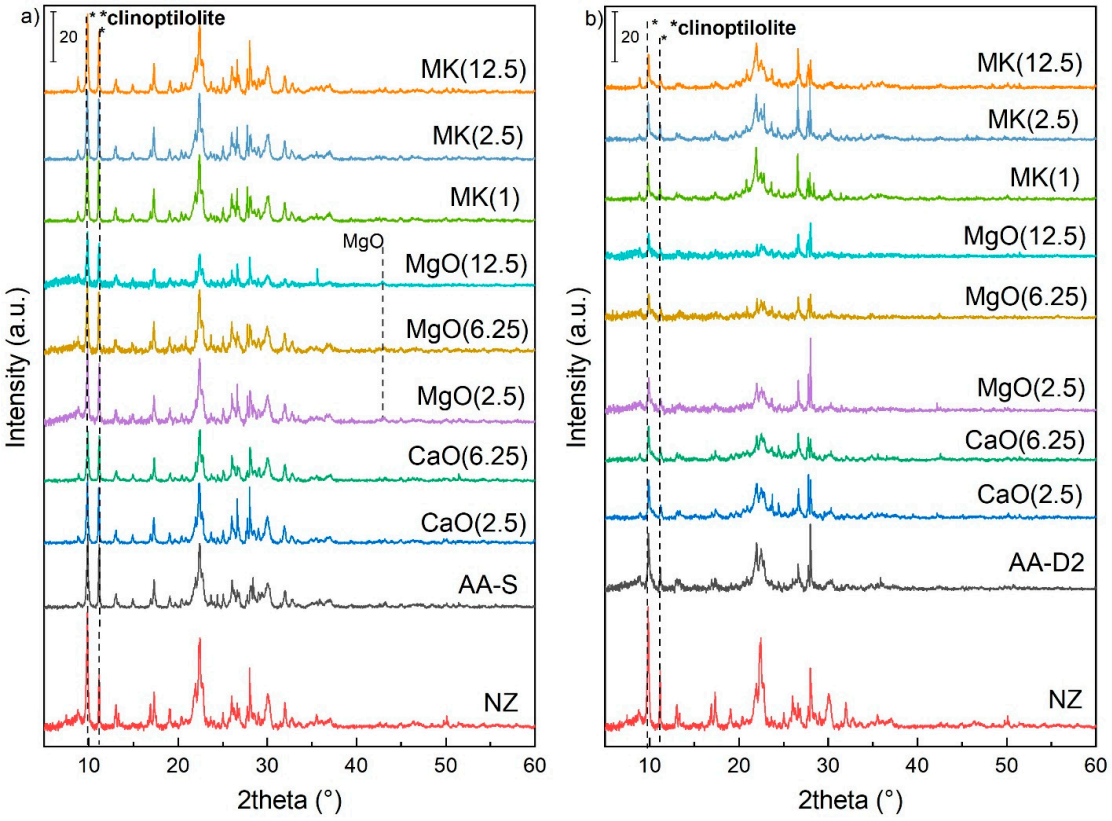

Figure 3. Diffractograms of "S" (**a**) and "D2" (**b**) samples series.

Table 2. Crystallinity and the intensity ratio of samples series "S" and "D2".

Sample	S			D2		
	Crystallinity [020] *	Crystallinity [200] **	Intensity Ratio [200]/[020]	Crystallinity [020] *	Crystallinity [200] **	Intensity Ratio [200]/[020]
NZ	168	93	0.48	73	44	0.20
AA	100	100	0.86	100	100	0.36
MgO(2.5)	103	92	0.77	60	54	0.33
MgO(6.25)	95	99	0.90	43	37	0.31
MgO(12.5)	64	53	0.71	42	35	0.30
CaO(2.5)	89	94	0.91	66	63	0.34
CaO(6.25)	67	78	0.99	62	67	0.39
MK(2.5)	102	104	0.88	66	69	0.38
MK(6.25)	111	111	0.86	68	73	0.39
MK(12.5)	112	102	0.78	61	56	0.33

* [020] = 9.9° 2θ, % vs. AA; ** [200] = 11.2° 2θ, % vs. AA.

Partially replaced by CaO, MgO, and MK samples leached using 3 M HCl showed a significant decrease in both intensities [020,200]. The most substantial decrease in crystallinity of D2 samples was in MgO(12.5) and MgO(6.25) by approximately 60%, which showed a strong attack of concentrated acid on the aluminosilicate framework (Table 2). Natural zeolite had a relative intensity ratio (11.2°/9.9° 2θ) of 0.5. In the case of prepared zeolite foam (sample AA-S), this ratio increased up to 0.9 due to the presence of alkali (Na, K). When the natural zeolite was partially replaced by MgO, CaO, and MK, this ratio varied between 0.7–1. There was a decrease in the ratio with the increasing MgO or CaO content in the mixture, which may be due to the presence of another phase (CSH or MSH) that covers the surface of the zeolite. Using 3 M HCl, the ratio of modified samples decreased to 0.3 and 0.4 (Table 2), indicating the purification of the zeolite structure from alkali.

The textural properties were determined by N_2 physisorption measurement (micro- and mesopore determination) and by Hg porosimetry (macro- and mesopore determination). Using a combination of

these techniques allowed characterization of the texture properties over a very wide range of pore sizes from 0.75 nm to hundreds of microns. Certain limits are given by the different measurement principles, but both techniques make it possible to determine mesopores.

The results of Hg porosimetry showed that all samples contained mesopores (2–50 nm) and macropores (>50 nm). The increase in the mesopore volume was visible in all CaO, MgO, and MK modified samples (Figure 4). The most visible increase of the pore volume in the mesoporous region was in the CaO(2.5) and CaO(6.25) samples (Figure 4a), even in leached samples (Figure 4b). In the case of MgO samples, there was only a slight increase of mesopore volume, but there was a very significant increase in the macropore volume in the 300–3000 nm region. The leaching using 3M HCl caused a decrease of pore volume in the 300–3000 nm region. Significant increases in the macropore volume in the region from 3000 nm were in MK(2.5) and MK(6.25) samples both before and after leaching.

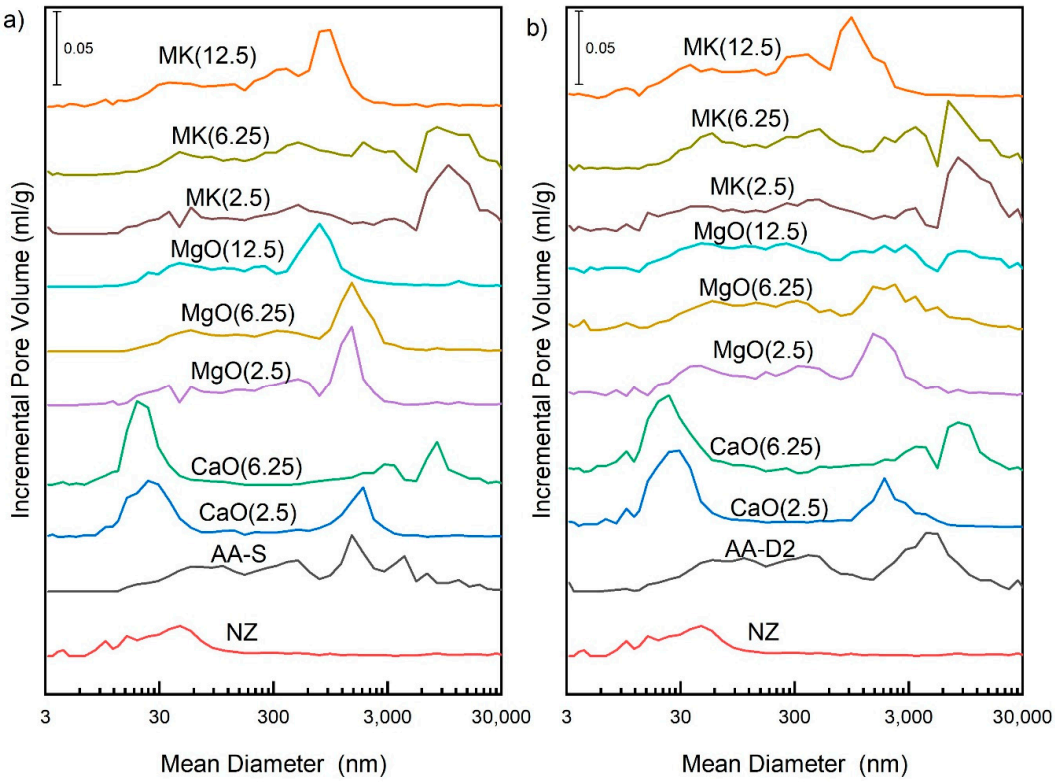

Figure 4. Hg porosimetry of "S" (**a**) and D2 (**b**) samples series.

N_2 physisorption is the most common technique for studying the surface area and size of mesopores and micropores in zeolites. The shape of the adsorption and desorption isotherm is important to obtain information on whether mesopores are present in the sample and what their shape is [16]. According to the International Union of Pure and Applied Chemistry (IUPAC) classification, we have identified the type of isotherm and thus the nature of the adsorption process. Thanks to the classification, it is possible to distinguish six types of isotherms for gas/solid equilibria [17]. The curves for the N_2 adsorption and desorption of D2 samples are presented in Figure 5a. The sample AA-S, which had very low mesoporosity and no micropores gave a type IV isotherm, while after the formation of mesopores and micropores and (in the case of modified D2 samples) a combination of type I and IV isotherms was observed. In the modified D2 samples, the presence of a hysteresis loop was evident, which indicates the occurrence of mesopores. Depending on the shape of the hysteresis loop, it is also possible to determine the shape of the mesopores [16]. IUPAC recommends dividing hysteresis loops into four types. In the CaO(2.5)-D2 and CaO(6.25)-D2 samples the type H3 of hysteresis was observed. The type H3 of hysteresis loop occurs with aggregates of plate-like particles, which lead to the formation of slit-shaped pores [18]. The MgO and MK modified samples showed the type H4. Type H4 loop

is generally related to narrow slit-like pores [18]. Most isotherms showed so-called low-pressure hysteresis—open isotherm (Figure 5a). This hysteresis can be caused by several different effects. Most often this type of hysteresis is caused by a change in the adsorbent volume by 'swelling/inflating' the pores in flexible or not rigid materials. Another cause may be irreversible adsorption of adsorptive molecules in pores of a size comparable to that of adsorptive molecules. The reason may also be insufficient steady state equilibrium if desorption and adsorption are significantly slowed by difficult diffusion of molecules through structural pores, especially in the area of microporosity [19].

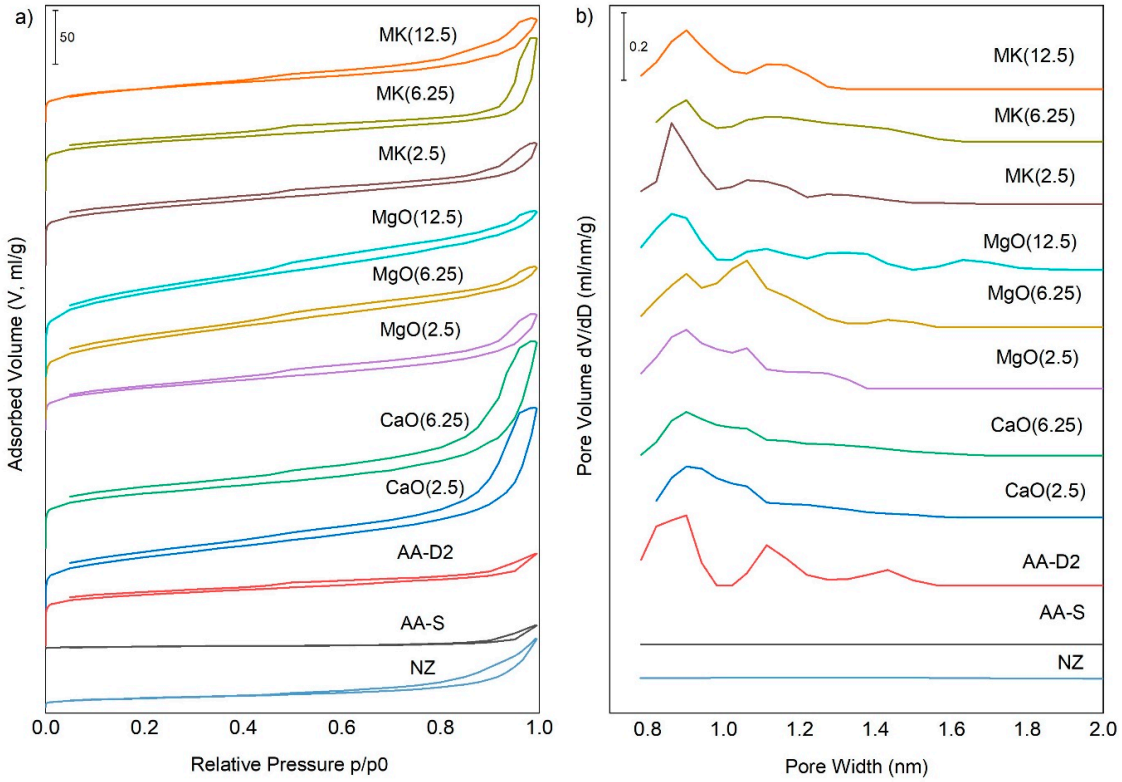

Figure 5. Nitrogen adsorption and desorption isotherms (**a**) and the distribution of micropores (**b**) of D2 samples.

The results of BET measurement showed that specific surface area for AA-S sample was only 7.1 m^2/g (Table 3). By partial replacement of natural zeolite and subsequent leaching, the surface increased up to 288.2 for MgO and 220.4 for CaO.

The specific surface area of the samples with metakaolin was lower and there was a decrease with an increasing amount of MK in the mixture. This was probably due to the formation of an amorphous geopolymer phase resulting from the dissolution of a portion of MK in the alkaline activator and its subsequent condensation. The resulting new phase partially blocked the pores. This was the opposite trend compared to CaO and especially MgO where was an increase in specific surface area with increasing amounts of CaO or MgO in the mixture. The increase was most likely due to the formation of hydrated Ca and Mg silicates in the structure of the material. The total pore volume of the AA-S sample (Table 3) was only 0.029 cm^3/g. By the subsequent leaching, the total pore volume increased four times to the value of 0.128 cm^3/g. The total pore volume of modified D2 samples varied between 0.119–0.268 cm^3/g. The greatest increase was observed in CaO samples and in MgO samples. While in the non-treated sample (AA-S) hardly any mesoporosity can be observed, in the modified D2 samples was a considerable increase in the mesopore volume, especially for the CaO and MgO samples. The presence of MgO and CaO in the initial mixture, after acid leaching, plays a significant role in building the mesoporous structure of the material. Ca and Mg are easily extractable

by acid and after their removal, additional pores are formed in the structure. By removing Ca and Mg, the aluminosilicate framework is easier to access and aluminum is better removed [20].

Table 3. Textural properties of D2 samples determined by N_2 physisorption measurement.

Sample	Surface Area-BET (m^2/g)	Total Pore Area (m^2/g) *	Total Pore Volume (cm^3/g) *	Micropore Volume (cm^3/g) *	Mesopore Volume (cm^3/g) *	Mesopore Volume 3–50 nm (cm^3/g) **
AA-S	7.1	6.0	0.029	0.000	0.024	0.047
AA	188.8	281.9	0.128	0.057	0.065	0.076
CaO(2.5)	220.4	298.6	0.268	0.049	0.194	0.290
CaO(6.25)	179.8	225.5	0.249	0.039	0.186	0.289
MgO(2.5)	231.1	316.5	0.207	0.054	0.144	0.120
MgO(6.25)	274.0	349.3	0.207	0.062	0.139	0.104
MgO(12.5)	288.2	395.9	0.233	0.061	0.166	0.124
MK(2.5)	188.8	253.9	0.153	0.045	0.099	0.101
MK(6.25)	147.3	210.0	0.119	0.038	0.076	0.090
MK(12.5)	191.9	267.0	0.184	0.044	0.130	0.125

* The total pore area, microporous and mesoporous volumes were determined by NLDFT; ** Mesopore volume 3–50 nm (cm^3/g) determined by Hg porosimetry.

Acid leaching, besides the formation of mesopores, also influenced the microporous structure. During the leaching, the pores blocked by cations were cleaned. This claim is well seen in Figure 5b where AA-S sample contained no micropores; however, the micropore distribution determined by N_2 physisorption (NLDFT method) showed a slight increase of micropores in all D2 samples.

The data from the cutting edge strength measurement showed that the cutting edge strength of the modified natural zeolite by CaO and MgO was significantly increased up to two times (Figure 6a). The only exception was the CaO(6.25) sample, there was a slight decrease in the strength compared to the AA-S sample.

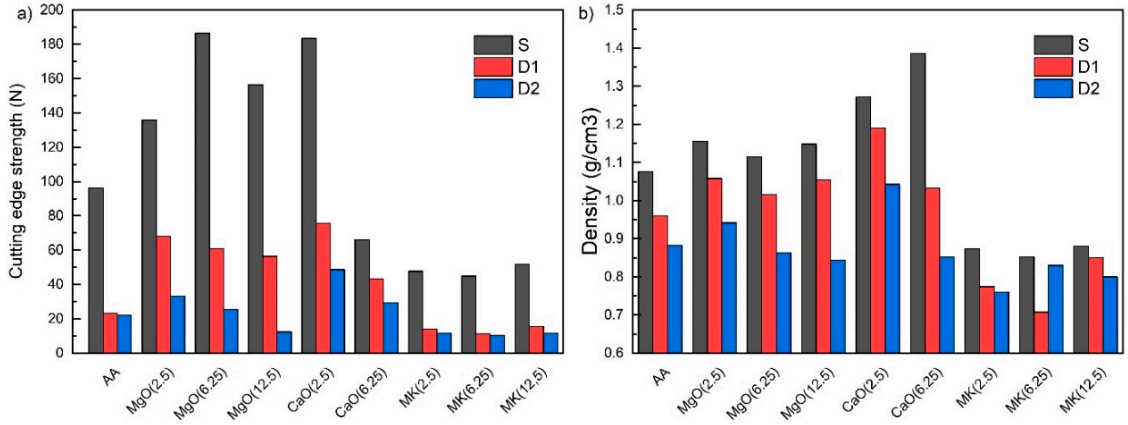

Figure 6. Cutting edge strength (**a**) and density (**b**) of all samples.

This decrease was caused by mechanical damage of the sample due to the 'tearing' that occurred during the shaping of the sample (pellet). The reaction of CaO with the silicate present in the alkaline activator was very rapid in contrast to MgO. With a small CaO addition (up to approx. 2.5 %), the effect on the mixture processing was not apparent. At a higher CaO addition, the rate of solidification was too high and during the processing of the mixture and subsequent shaping of the solidifying sample so-called tearing of the sample occurred. The subsequent foaming led to further stressing of the damaged and partially solidified mixture because the H_2O_2 decomposition process was slower than solidification. For this reason, it was not possible to prepare a sample with a higher CaO content (12.5%) because the prepared mixture solidified during the preparation in the dish.

On the other hand, the data showed that the strength of the natural zeolite modified by MK decreased two times and the strength was decreasing with the increasing amount of MK in the mixture.

This decrease was due to the insufficient formation of the N(K)-A-S-H phase. In this case, the phase was not perfectly crosslinked and did not increase the strength of the material. For alkaline activation of MK (preparation of geopolymers), a different composition of the alkaline activator is required for optimal geopolymerization. Metakaolin geopolymers require a lower mass ratio of Na_2SiO_3/KOH (lower Na_2SiO_3 content) because high demands on water in addition to the increased in the Na_2SiO_3 content increase the stickiness of the mixture and thus decrease its processability [11].

The strength of D2 samples decreased to values below 20 N, however, the strength of the D2 samples with the low CaO and MgO content was higher than without the addition of these additives. On the other hand, a decrease in higher MgO and CaO contents was observed, which was caused by a significant increase in specific surface area or pore volume. These two parameters (strength vs. porosity) always go against each other.

The decrease after high concentrated acid leaching is related especially to the removal of the excess alkaline activator in the pores, which strengthened the material and removing other components associated with the formation of additional pores [13]. Modification of the natural zeolite by CaO and MgO also increased the density to 1.1–1.4 g/cm^3 (Figure 6b). Whereas, in the case of MgO, the increase of the density was slight in the case of CaO, the increase was quite significant. This could be related to the observed differences in the prepared pellets, which in the case of CaO were shorter and less foamed. The reason may be a higher rate of solidification of the mixture, which the oxygen, formed during the decomposition of H_2O_2, can no longer foam.

In contrast, the density of the modified zeolite by MK decreased due to the reduction of the viscosity of the mixture by the addition of MK.

The amount, type and strength of acid sites on the surface of D2 samples plays a crucial role in promoting catalytic activity [21] and thus the acidity was determined by temperature-programmed ammonia desorption (NH_3-TPD). It can be seen from Figure 7, that the TPD curves contained a dominant low-temperature peak with a center between 148 °C and 172 °C. This temperature maximum is related to the ammonia desorption at weakly acidic Lewis sites. Samples modified with MgO had temperature peaks slightly shifted to lower temperatures compared to the AA-D2 sample and samples modified with CaO and MK. The AA-D2 sample had the lowest Si/Al ratio and on the other hand, MgO modified samples had the highest Si/Al ratio. As stated in the study by Wang et al. (2013) [21], the acid strength of zeolites is associated with the Si/Al molar ratio. This statement is supported by our results, which showed that the lower the Si/Al ratio, the higher the acid strength of zeolite modified MK samples show the lowest concentration of low-temperature acid sites, especially the sample MK(6.25) which has the concentration of low-temperature acid sites just 0.204 mmol/g. (Table 4).

Table 4. Acidity of D2 zeolite foam pellets determined by the NH_3-TPD

Sample	T_{max} (°C)	c_{LT} (mmol/g)
AA	172	0.336
MgO(2.5)	155	0.347
MgO(6.25)	148	0.290
MgO(12.5)	148	0.316
CaO(6.25)	166	0.341
CaO(2.5)	160	0.294
MK(2.5)	167	0.280
MK(6.25)	162	0.204
MK(12.5)	164	0.229

*T*max—temperature maximum (°C); cLT—concentration of low-temperature acid sites (mmol/g).

Zeolitic materials were investigated, which are mainly used in the construction industry as a supplementary cementitious material. For their wider use, our previous study tested acid and thermal treatment of alkali activated zeolite foams [13]. Following this study, we modified the natural zeolite

by the addition of CaO, MgO, and MK and observed the effect of these additives on the material properties. According to the measured data, these additives significantly improved the properties of alkali activated zeolite foams (especially the specific surface area and strength), making these foams a very promising material for the future use in other industries. These materials have been studied intensively for a long time and direct catalytic applications have been presented. A detailed examination of these materials is now ongoing and the main objective will be to promote these cheap and easy to manufacture materials to the industrial scale.

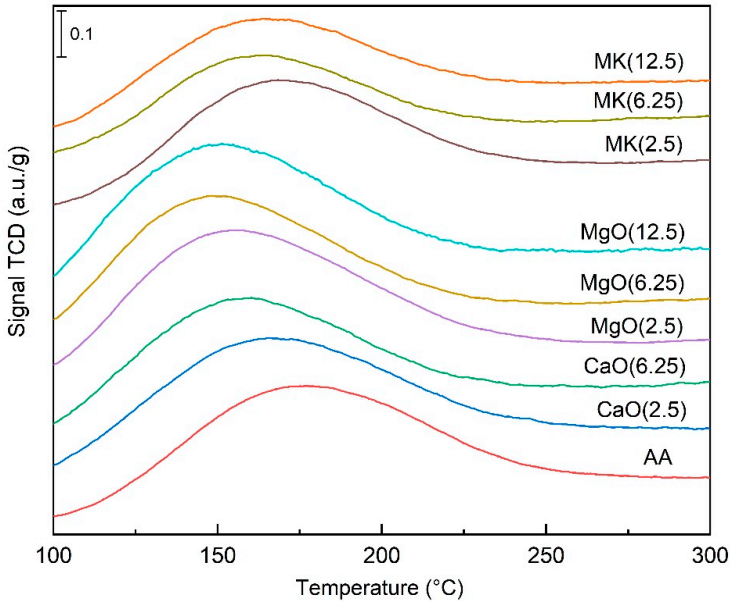

Figure 7. NH_3-TPD of modified D2 samples.

4. Conclusions

In this work, natural zeolite containing clinoptilolite was modified with MgO, CaO, and MK, then alkali activated (KOH solution with sodium silicate), foamed using H_2O_2, and subsequently leached using 0.1 M and 3 M HCl. The basic alkali activated zeolite foam was compared with MgO, CaO, and MK modified alkali activated foams. There was investigated the effect of the natural zeolite modification and subsequent leaching on the textural, chemical and mechanical properties of materials. Properties of modified natural zeolite were determined by N_2 physisorption, Hg porosimetry, NH_3-TPD, XRF, XRD, and strength analyses.

The XRF analysis showed that the highest Si/Al ratio had samples modified with CaO and MgO and subsequently leached using 3 M HCl. The Si/Al ratio is also related to the occurrence of mesopores. It was demonstrated by the N_2 physisorption and Hg porosimetry measurement that the largest increase in mesopore was in the samples with the highest Si/Al ratio. As a result of acid leaching, the accompanying elements (Al, K, Na, Ca, Mg, Fe) were removed so the pores (especially micropores) were perfectly cleaned, causing an increase of micropore volume, mesopore volume and total pore volume. There was a significant increase in the surface area too. The modification by MgO and subsequent leaching, the surface increased by almost 300 m^2/g.

Very surprising results were obtained by analysis of strength, which showed that the modification of natural zeolite by CaO and MgO led to a double increase of strength. After acid leaching, there was a decrease of strength related to the removal of the excess alkaline activator in the pores, but for CaO and MgO modified samples, the decrease is significantly lower.

The NH_3-TPD analysis showed that the lowest acidity had MgO modified samples because of the high Si/Al ratio where the substitution of Al atoms decreases the acid strength of zeolite.

The results of the analysis showed that there was an improvement in important properties, especially in the increase of pore volume, surface area, and in the cutting edge strength. These improved parameters can lead to an extension of the potential applicability of alkali activated zeolite foams in the chemical industry, especially in catalytic and sorption applications.

Author Contributions: Conceptualization, Z.T.; Methodology, Z.T.; Validation, K.H. and J.Š.; Formal analysis, K.H. and J.Š.; Investigation, J.Š. and K.H.; Writing—original draft preparation, K.H..; Writing—review and editing, Z.T. and E.S.; Visualization, E.S. and K.H.; Supervision, Z.T. All authors have read and agreed to the published version of the manuscript.

Funding: The publication is a result of the project Development of the UniCRE Centre (project code LO1606) which has been financially supported by the Ministry of Education, Youth and Sports of the Czech Republic (MEYS) under the National Sustainability Programme I. The result was achieved using the infrastructure of the project Efficient Use of Energy Resources Using Catalytic Processes (LM2015039) which has been financially supported by MEYS within the targeted support of large infrastructures.

Conflicts of Interest: The authors declare no conflict of interest. The funders had no role in the design of the study; in the collection, analyses, or interpretation of data; in the writing of the manuscript, or in the decision to publish the results.

Appendix A

Table A1. Chemical composition of samples.

Sample			SiO_2	Al_2O_3	K_2O	Fe_2O_3	CaO	Na_2O	MgO	TiO_2	SUM
AA		S	71.20	10.50	8.71	1.37	3.25	3.84	0.72	0.16	99.75
		D1	78.60	11.20	5.36	1.40	1.88	0.56	0.55	0.19	99.74
		D2	89.50	6.84	1.26	0.95	0.62	0.25	0.33	0.19	99.93
MgO	(2.5)	S	69.90	10.30	8.45	1.24	3.07	3.61	3.11	0.17	99.85
		D1	74.90	10.90	6.31	1.36	2.57	0.92	2.69	0.18	99.83
		D2	91.30	5.18	1.36	0.89	0.53	0.24	0.26	0.18	99.95
	(6.25)	S	67.10	9.83	8.52	1.28	2.94	3.46	6.45	0.16	99.74
		D1	72.60	10.50	6.33	1.35	2.53	1.01	5.26	0.18	99.76
		D2	92.00	4.57	1.28	0.86	0.49	0.27	0.30	0.19	99.96
	(12.5)	S	63.50	9.32	8.05	1.16	2.63	3.42	11.50	0.15	99.73
		D1	69.10	9.93	6.11	1.27	2.52	1.06	9.69	0.17	99.85
		D2	92.30	4.25	1.26	0.88	0.52	0.22	0.36	0.18	99.97
CaO	(2.5)	S	69.80	9.87	8.80	1.33	4.90	4.32	0.61	0.16	99.79
		D1	76.00	10.70	6.21	1.36	3.89	0.85	0.59	0.17	99.77
		D2	90.80	5.39	1.33	0.93	0.65	0.25	0.25	0.18	99.78
	(6.25)	S	66.80	9.26	9.47	1.29	7.78	4.42	0.59	0.16	99.77
		D1	74.50	10.20	6.04	1.32	6.11	0.80	0.58	0.17	99.71
		D2	91.80	4.61	1.30	0.86	0.63	0.25	0.22	0.19	99.87
MK	(2.5)	S	71.10	11.10	8.23	1.37	3.17	3.66	0.67	0.18	99.47
		D1	76.30	12.00	6.08	1.44	2.13	1.10	0.54	0.19	99.78
		D2	91.10	5.36	1.39	0.97	0.51	0.23	0.25	0.19	100.01
	(6.25)	S	70.10	12.60	8.34	1.32	3.00	3.59	0.66	0.19	99.80
		D1	76.60	13.00	5.57	1.41	1.90	0.61	0.50	0.19	99.78
		D2	91.40	5.19	1.27	0.92	0.51	0.21	0.25	0.21	99.95
	(12.5)	S	69.60	13.00	8.19	1.31	2.90	3.65	0.65	0.20	99.50
		D1	75.20	14.20	5.58	1.34	1.98	0.70	0.54	0.21	99.75
		D2	90.60	5.96	1.27	0.89	0.50	0.24	0.25	0.23	99.94

References

1. Wang, S.; Peng, Y. Natural zeolites as effective adsorbents in water and wastewater treatment. *Chem. Eng. J.* **2010**, *156*, 11–24. [CrossRef]
2. Mar Camacho, L.; Deng, S.; Parra, R.R. Uranium removal from groundwater by natural clinoptilolite zeolite: Effects of pH and initial feed concentration. *J. Hazard. Mater.* **2010**, *175*, 393–398. [CrossRef] [PubMed]

3. Motsi, T.; Rowson, N.A.; Simmons, M.J.H. Adsorption of heavy metals from acid mine drainage by natural zeolite. *Int. J. Miner. Process.* **2009**, *92*, 42–48. [CrossRef]
4. Englert, A.H.; Rubio, J. Characterization and environmental application of a Chilean natural zeolite. *Int. J. Miner. Process.* **2005**, *75*, 21–29. [CrossRef]
5. Ahmadi, B.; Shekarchi, M. Use of natural zeolite as a supplementary cementitious material. *Cem. Concr. Com.* **2010**, *32*, 134–141. [CrossRef]
6. Ramezanianpour, A.A.; Mousavi, R.; Kalhori, M.; Sobhani, J.; Najimi, M. Micro and macro level properties of natural zeolite contained concretes. *Constr. Build. Mater.* **2015**, *101*, 347–358. [CrossRef]
7. Tišler, Z.; Horáček, J.; Šafář, J.; Velvarská, R.; Pelíšková, L.; Kocík, J.; Gherib, Y.; Marklová, K.; Bulánek, R.; Kubička, D. Clinoptilolite foams prepared by alkali activation of natural zeolite and their post-synthesis modifications. *Microporous Mesoporous Mater.* **2019**, *282*, 169–178. [CrossRef]
8. Groen, J.C.; Brouwer, S.; Peffer, L.A.A.; Pérez-Ramírez, J. Application of Mercury Intrusion Porosimetry for Characterization of Combined Micro- and Mesoporous Zeolites. *Part. Part. Syst. Charact.* **2006**, *23*, 101–106. [CrossRef]
9. Król, M.; Rożek, P.; Chlebda, D.; Mozgawa, W. ATR/FT-IR studies of zeolite formation during alkali-activation of metakaolin. *Solid State Sci.* **2019**, *94*, 114–119. [CrossRef]
10. Wahono, S.K.; Prasetyo, D.J.; Jatmiko, T.H.; Pratiwi, D.; Suwanto, A.; Hernawan; Vasilev, K. Multi-stage dealumination for characteristic engineering of mordenite-clinoptilolite natural zeolite. *AIP Conf. Proc.* **2019**, *2085*, 020044.
11. Heah, C.Y.; Hussin, K.; Al Bakri, A.M.; Hussain, R.R.; Luqman, M.; Nizar, I.K.; Ghazali, C.M.R.; Liew, Y.M. Study on solids-to-liquid and alkaline activator ratios on kaolin-based geopolymers. *Constr. Build. Mater.* **2012**, *35*, 912–922. [CrossRef]
12. Khale, D.; Chaudhary, R. Mechanism of geopolymerization and factors influencing its development: A review. *J. Mater. Sci.* **2007**, *42*, 729–746. [CrossRef]
13. Tišler, Z.; Hrachovcová, K.; Svobodová, E.; Šafář, J.; Pelíšková, L. Acid and Thermal Treatment of Alkali-Activated Zeolite Foams. *Minerals* **2019**, *9*, 719. [CrossRef]
14. Walkley, B.; Nicolas, R.S.; Sani, M.A.; Rees, G.J.; Hanna, J.V.; Van Deventer, J.S.J.; Provis, J. Phase evolution of C-(N)-A-S-H/N-A-S-H gel blends investigated via alkali-activation of synthetic calcium aluminosilicate precursors. *Cem. Concr. Res.* **2016**, *89*, 120–135. [CrossRef]
15. Vegere, K.; Vitola, L.; Argalis, P.P.; Bajare, D.; Krauklis, A.E. Alkali-Activated Metakaolin as a Zeolite-Like Binder for the Production of Adsorbents. *Inorganics* **2019**, *7*, 141. [CrossRef]
16. Van Donk, S.; Janssen, A.H.; Bitter, J.H.; De Jong, K.P. Generation, Characterization, and Impact of Mesopores in Zeolite Catalysts. *Catal. Rev.* **2003**, *45*, 297–319. [CrossRef]
17. Donohue, M.; Aranovich, G. Classification of Gibbs adsorption isotherms. *Adv. Colloid Interface Sci.* **1998**, *76*, 137–152. [CrossRef]
18. Tang, X.; Jiang, Z.; Li, Z.; Gao, Z.; Bai, Y.; Zhao, S.; Feng, J. The effect of the variation in material composition on the heterogeneous pore structure of high-maturity shale of the Silurian Longmaxi formation in the southeastern Sichuan Basin, China. *J. Nat. Gas Sci. Eng.* **2015**, *23*, 464–473. [CrossRef]
19. Bulánek, R. Povrchové jevy na pevných látkách, 1st ed. Univerzita Pardubice; pp. 1–118. Available online: https://e-shop.upce.cz/img/img.fpl?id_img=9004680&size=full (accessed on 2 April 2020).
20. Groen, J.C.; Jansen, J.C.; Moulijn, J.A.; Pérez-Ramírez, J. Optimal Aluminum-Assisted Mesoporosity Development in MFI Zeolites by Desilication. *J. Chem. Soc. B* **2004**, *108*, 13062–13065. [CrossRef]
21. Wang, N.; Zhang, M.; Yu, Y. Distribution of aluminum and its influence on the acid strength of Y zeolite. *Microporous Mesoporous Mater.* **2013**, *169*, 47–53. [CrossRef]